JPIChE 49 (1) 2021: 11-20

Journal of Pakistan Institute of Chemical Engineers

Since 1969

journal homepage: www.piche.org.pk/journal

Surface Modification of AZ31B Magnesium Alloy by Anodization Process

*F. Hussain**[1], M. U. Manzoor[1], M. Kamran[1], M. T. Z. Butt[1]*

Submitted: 05/03/2021, Accepted: 29/03/2021, Online: 30/03/2021

Abstract

Magnesium alloys emerge as a new class of biomaterials in medical field especially in orthopedic applications as medical implant because of its excellent mechanical, biocompatible, bioactive and biodegradable properties. Biodegradable magnesium alloys have attracted great attention of researchers to avoid implant removal surgery after healing process. The magnesium alloy samples were anodized in two different electrolyte solutions to further improve the biodegradability of the substrates. The processing time varies from 10 minutes to 40 minutes with constant voltage of 20V. Coated samples were characterized with scanning electron microscopy (SEM) for surface topography and energy dispersive x-ray spectroscopy (EDX) which confirmed the deposition of thick and dense oxide layers of anodized film of magnesium oxide (MgO) and magnesium hydroxide $Mg(OH)_2$ in electrolyte 2. The results of electrochemical Impedance spectroscopy (EIS) are in a good agreement with the analyses of surface morphology. The anodic film formed by electrolyte 2 provides better biodegradability as compared to that of formed by electrolyte 1.

Keywords: AZ31B Magnesium Alloy, Anodization, Energy Dispersive X-Ray Spectroscopy**,** Electrochemical Impedance Spectroscopy, Scanning Electron Microscopy

1. Introduction:

Magnesium alloys have attracted considerable importance for the last decade because of its biocompatible, bioactive and biodegradable properties and are used as a bioresorbable implant material. Human bone consists of hydroxyapatite as a main component. This composite material is not strong enough to bear high impact like other metallic materials. In case of bone breakage or hip joint replacement, the alignment of bone is a very crucial stage and this alignment is done with the help of screws and plates made of biomaterials. The metallic biomaterials are preferably used because of their excellent mechanical and biocompatible properties. Biomaterials differ from other materials because of their ability to remain in a physiological environment without damaging the surrounding and without getting damaged in the process [1-5]. Biocompatibility is a property of a biomaterial that it will perform effectively with the host response for the desired application while working within the physiological environment. Initially cobalt chromium alloys were used as an implant material for their good mechanical and biocompatible properties. Stainless steel was then used because of low density than cobalt chromium alloy and better biodegradable properties. Stainless steel was replaced by titanium and its alloys because of even better mechanical and biocompatible properties. In all the above mentioned biomaterials, degradation of the material in human physiological environment

[1]Institute of Metallurgy & Materials Engineering, Faculty of Chemical & Materials Engineering, Quaid-e-Azam Campus, University of the Punjab, 54590. Lahore, Pakistan,
Corresponding Author: faraz.imme@pu.edu.pk

is inevitable. The material starts to degrade within the body with the passage of time. The second surgery for the removal of implant from the human body that is covered with the muscles and tissues in that particular place is inexorable and this leads to unbearable pain for the patient and turns out to be an expensive treatment as well [6-11].

Bioresorbable materials are the biocompatible materials that are gradually resorbed within the body. Magnesium and its alloys have a particular such property that make it a choice of material for an implant application. Pure Magnesium metal and its alloys are also prone to localized corrosion in a physiological environment [12-16] accompanied by the hydrogen gas evolution and leads to cavities of hydrogen gas in tissues [17, 18]. Magnesium and its alloys in aqueous environment produce magnesium hydroxide and hydrogen gas [19] as shown in equations 1-3.

$$Mg \rightarrow Mg^{+2} + 2e^{-} \quad (1)$$

$$2H_2O + 2e^{-} \rightleftarrows 2OH^{-} + H_2 \quad (2)$$

$$Mg + 2H_2O \rightleftarrows Mg(OH)_2 + H_2 \quad (3)$$

Addition of alloying elements, mechanical pre-processing and surface modification are the main treatments to minimize the effect of corrosion [20, 21]. Anodization is an electrolytic oxidation technique in which the metal surface acting as anode, is changed to its oxide forming a film on the surface possessing preferable functional, decorative and corrosion protective properties. Anodized film can provide better adhesion and enhance the corrosion, wear resistance and hardness. The anodizing parameters have great influence on the anodized film. Several researchers have investigated the effect of pre and post treatments, electrolyte composition, treatment time and electrical parameters on the morphology of anodized films [22-27]. Researchers have also worked on eco-friendly anodizing processes. Lei et al. [28, 29] investigated the anodization of Magnesium alloys in concentrated 6M and 10M KOH solution by potentiostatic technique followed by annealing. The results showed that Magnesium alloys coated with magnesium oxide exhibited better corrosion resistance properties as compared to non-anodized magnesium alloy. The 6M electrolytic solution developed magnesium oxide (MgO) layer whereas 10M solution produced magnesium hydroxide ($Mg(OH)_2$) coating followed by calcination to produce MgO coating. The as grown coating showed better corrosion resistance properties in Hank's solution as compared to bare metallic magnesium.

Xue et al. [30] investigated that the corrosion resistance was increased by anodization of both pure Mg and AZ91D and the anodization time had a great influence on the corrosion resistance. Chai et al. [31] showed that the corrosion resistance of anodic layer was closely associated with applied current density. By applying high current density, porous surface and strong corrosion resistance of anodic films were achieved. The temperature of solution had an adverse effect on the anti-corrosion characteristic of anodic layer with current density. Ximei et al. [25] studied that the anodic layer formed on the AZ91D Mg alloy pretreated in solution of aluminium nitrate with or without ultrasonification. This enhanced the AZ91D Mg alloy corrosion resistance more expressively than that without pretreatment in solution of aluminium nitrate. Fukuda et al. [23] examined that anodic films formed on AZ91D in 3 M KOH solutions with and without addition of 0.55 M Na_2SiO_3. The anodic films formed in 3 M KOH solutions with the addition of Na_2SiO_3 were thicker and more even than the layers formed in the absence of sodium silicate.

The above cited literature shows that most of the work was performed in potassium hydroxide (KOH) solution. The aim of this preset research was to compare the anodization potential of the two different types of alkaline electrolytes to anodize AZ31B magnesium alloy and optimize for these electrolyte's processing time to obtain anodized film. This type of comparison is not reported in the literature. The surface morphology of the magnesium alloy was studied using scanning electron microscopy (SEM) and the chemical composition of anodized layer deposited on magnesium alloy was measured using energy

dispersive x-ray spectroscopy (EDX). Furthermore, electrochemical impedance spectroscopy curves were obtained in Ringer lactate solution to estimate the corrosion behavior of magnesium alloy.

2. Experimental Work:

2.1 Materials:

Commercially available sheet of AZ31B magnesium alloy was used as a substrate material for anodization process. The substrate with dimensions 1.5ft x 1.5ft x 5mm was purchased from Dongguan Feitai Metal Product CO. LTD., China. The composition of the magnesium alloy AZ31B is shown in table 1.

Table 1: Chemical composition of magnesium alloy AZ31B

Item	AZ31B Standard (%)	AZ31B Obtained (%)
Mg	Balance	Balance
Al	2.5-3.5	3.16
Mn	0.2-1.0	0.31
Si	0.08	0.035
Fe	0.003	0.0023
Zn	0.6-1.4	0.93
Cu	0.01	0.0015
Ni	0.001	0.00052

Square pieces of magnesium alloy substrate, used as working electrode, were cut from the as-received sheet using a wire cutting process to get a dimension of 10 mm x 10 mm x 5 mm. The specimens were drilled and then fixed with the copper wire. The samples were washed with ethanol and then embedded in the epoxy resin for complete insulation. The exposed surface of 10 mm by 10 mm dimensional area was abraded successively for grinding. The sample preparation method adopted in this study was as reported by Umar et al. [32]. The samples were then ultrasonically cleaned in acetone and ethanol prior to anodization.

2.2 Anodizing Procedure:

Anodization tests were carried out using a DC Power supply using the magnesium samples as the anode and the graphite sheet as cathode. The electrolytes used in this research is given as below in table 2.

Table 2: Chemical composition of electrolytes used

Chemical Name	
Electrolyte 1 Ethylene Glycol	**Electrolyte 2** Ethylene Glycol
Methanol	Potassium Hydroxide (KOH)
Ammonium Dihydrogen Phosphate ($(NH_4)H_2PO_4$)	Potassium Fluoride (KF)
Ammonium Fluoride (NH_4F)	Aluminium Nitrate ($Al(NO_3)_3$)
Potassium Hydroxide (KOH)	Sodium Silicate (Na_2SiO_3)
	Sodium Phosphate (Na_2PO_4)

The samples were anodized under four different processing times i.e. 10, 20, 30, and 40 minutes at constant voltage of 20V. Finally, the oxide films were rinsed using ethanol.

2.3 Characterization

Scanning Electron Microscopy (SEM) with EDX (*Mira 3 TESCAN USA*) was used to determine the coating thickness and chemical composition of the coating and surface morphologies of the coated samples. The corrosion behavior of the anodized samples was studied in Ringer lactate solution. The chemical composition of Ringer lactate solution is given in table 3.

Table 3: Composition of ringer lactate solution

Composition	g/L
NaCl	6.0
KCl	0.4
$CaCl_2.H_2O$	0.3
$C_3H_5NaO_3$ (50% sol.)	6.1
HCl (25% sol.)	0.2

Open Circuit Potential (OCP), Electrochemical Impedance Spectroscopy (EIS) and Cyclic Polarization tests were carried out using Potentiostat (*GAMRY interface 3000 USA*) on the anodized sample with different exposure time. A three-electrode system consisting of a reference electrode **"*Ag/AgCl*"**, a counter electrode (graphite) and the working electrode (magnesium sample) was used.

Open circuit potential was carried out after 1-day exposure time in Ringer lactate solution for 1800 sec. Electrochemical Impedance Spectroscopy was performed at 10 mV_{rms} w.r.t OCP and AC potential amplitude was kept within 0.01 Hz - 100 kHz frequency range.

2.4 Nomenclature:

The nomenclature of the tested samples is shown in table 4.

Table 4: Nomenclature of Electrolytes used

	Sample	Processing Time (minutes)
Electrolyte 1	Ano110	10
	Ano120	20
	Ano130	30
	Ano140	40
Electrolyte 12	Ano210	10
	Ano220	20
	Ano230	30
	Ano240	40

3. Results and Discussion:

3.1 Surface Morphology:

The scanning electron micrographs show the surface morphology of the anodized coating on AZ31B magnesium alloy with 30 minutes and 40 minutes of anodization at 20V in electrolyte 1 (Ano130 and Ano140) is shown in Figure1.

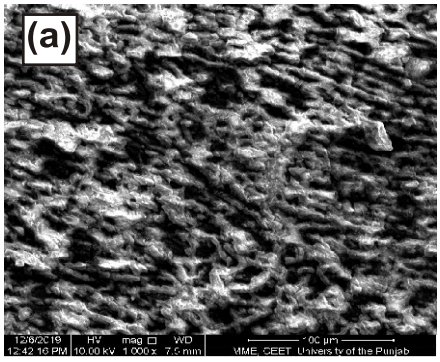

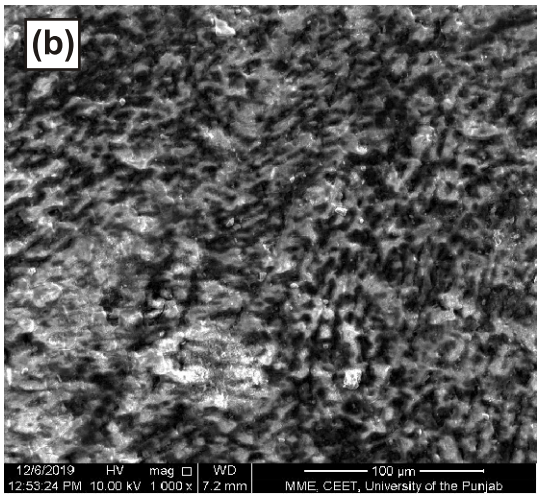

Figure 1: Scanning Electron Microscopy of surface morphology of anodized samples at 20V in electrolyte 1 at (a) 30 min (Ano130) and (b) 40 min (Ano140)

The surface morphology of the anodized coatings on AZ31B magnesium alloy with 30 minutes and 40 minutes of anodization at 20V in electrolyte 2 (Ano230 and Ano240) is shown in Figure2.

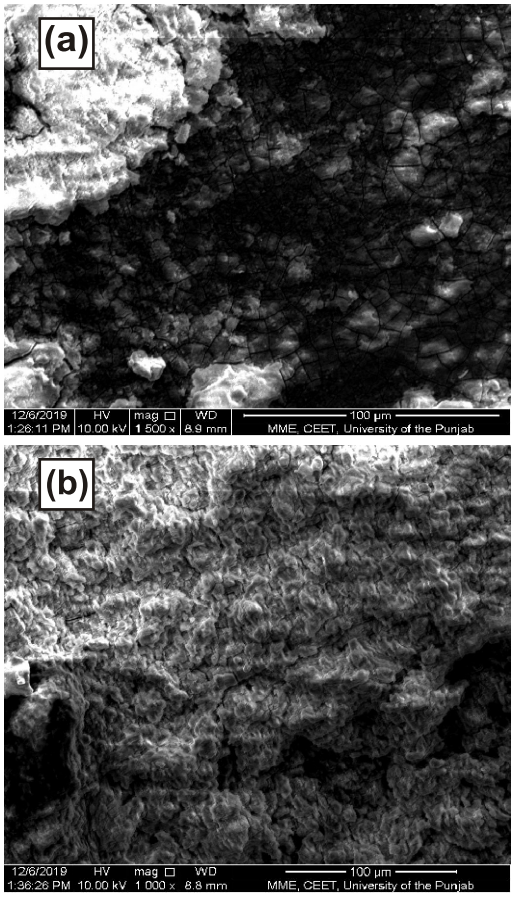

Figure 2: Scanning electron microscopy of surface morphology of anodized samples at 20V in electrolyte 2 at (a) 30 min (Ano230) and (b) 40 min (Ano240)

The micrographs of anodized samples formed in electrolyte 1 revealed irregular pores as clearly seen in micrograph 1 (a). The film formed in 30 minutes processing time (Figure 1a) is non-uniform and more porous. Whereas the film formed in 40 minutes processing time (Figure 1b), resulted in uniform layer as compare to that of 30 minutes. The diameter of the pores formed at 30 minutes (Fig 1a) is enormous than that of formed at 40 minutes (Figure 1b). When the treatment time is short, the surface morphology of the anodized film was smooth, uniform and contained large pores. With the increase of time, unbroken anodized film appeared with progressive decrease in pore size. The surface morphology of anodized layer formed in electrolyte 2 produced dense film having large number of micro-cracks as visible in Figure 2. The film formed at 30 minutes (Figure 2a) produced non-uniform and less dense layer along the substrate. The film formed at 40 minutes (Figure 2b) resulted in uniform and denser film along the sample. By increasing the time from 30 minutes to 40 minutes, compact and denser anodized film having micro-cracks are formed. Comparing both electrolytes, the anodized film formed in electrolyte 1 with different time periods produced uniform and less dense film having decrease in pore size while film formed in electrolyte 2 produced compact and denser film having large number of micro-cracks. The corrosion of the anodic layers is due to these large pores and micro-cracks [33].

3.2 Composition:

EDX analyses of the anodized samples with different processing time at constant voltage in electrolyte 1 and electrolyte 2 are shown in figure 3 and figure 4.

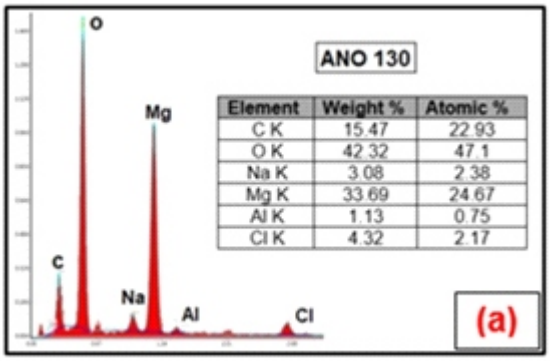

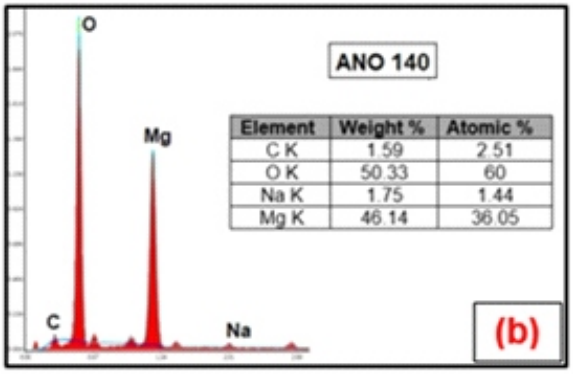

Figure 3: EDX analysis of anodized coating at 20V in electrolyte 1 at the treatment time of (a) 30 minutes (Ano130) and (b) 40 minutes (Ano140)

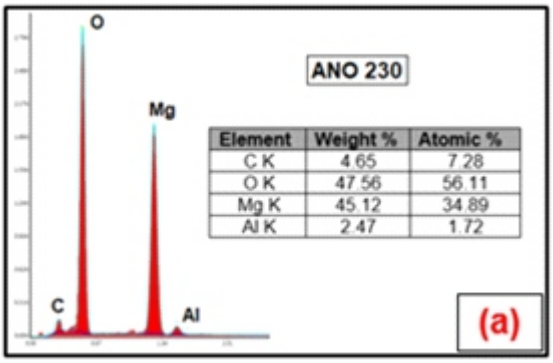

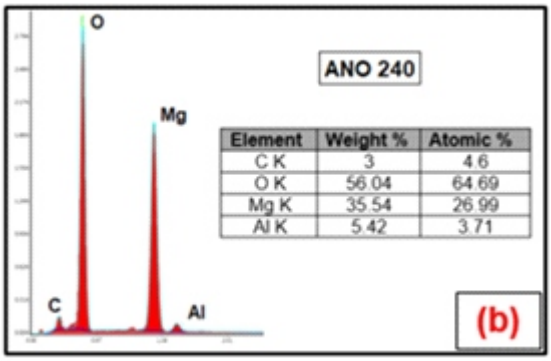

Figure 4: EDX analysis of anodized coating at 20V in electrolyte 2 at the treatment time of (a) 30 minutes (Ano230) and (b) 40 minutes (Ano240)

The surface morphology of the anodic layer showed a large number of irregular pores and micro-cracks which were distributed throughout the film. These pores and micro-cracks may provide routes for the electrolyte to reach the oxide/metal interface. The EDX investigation revealed that the anodic films comprised mostly of magnesium (Mg), aluminium (Al) and oxygen (O) which indicated the presence of magnesium oxide MgO and magnesium hydroxide

$Mg(OH)_2$ which were clearly seen in Figure 3 and Figure 4 [34].

EDX analyses of electrolyte 1 showed that the atomic and weight percentages of magnesium are higher for processing time of 40 minutes in comparison with processing time of 30 minutes. The atomic and weight percentages of oxygen are lower for 30 minutes as compared to 40 minutes. Analyses of electrolyte 2 revealed that the atomic and weight percentages of oxygen are lower for treatment time of 30 minutes whereas, these percentages are higher for treatment time of 40 minutes. The atomic and weight percentages of magnesium are higher for 40 minutes while these percentages are lower for that of having the processing time of 30 minutes. The higher percentages of magnesium and oxygen with processing time of 40 minutes in electrolyte 1 indicating the presence of more oxides of magnesium as compared to that of having the processing time of 30 minutes is clearly seen in Figure 1b. In electrolyte 2, higher percentages of magnesium and oxygen with processing time of 40 minutes signify the presence of more oxides of magnesium as compared to that of having the processing time of 30 minutes as is visible in Figure 2b. The presence of carbon and sodium in the analysis were from electrolytes.

By comparing both electrolytes, the anodic film formed in electrolyte 2 with the processing time of 30 minutes comprises of higher percentages of magnesium and oxygen, in the form of MgO and $Mg(OH)_2$, as compared to that of processing time of 30 minutes in electrolyte 1. The anodic film formed in electrolyte 2 with the processing time of 40 minutes comprises of higher percentages of magnesium and oxygen as compared to that of electrolyte 1 with processing time of 40 minutes.

3.3 Thickness:

Figure 5 showed coating thickness comparison of anodized coating on AZ31B magnesium alloy with different processing time at constant voltage of 20V in two different electrolytes and coating thickness variation in (%) at different time.

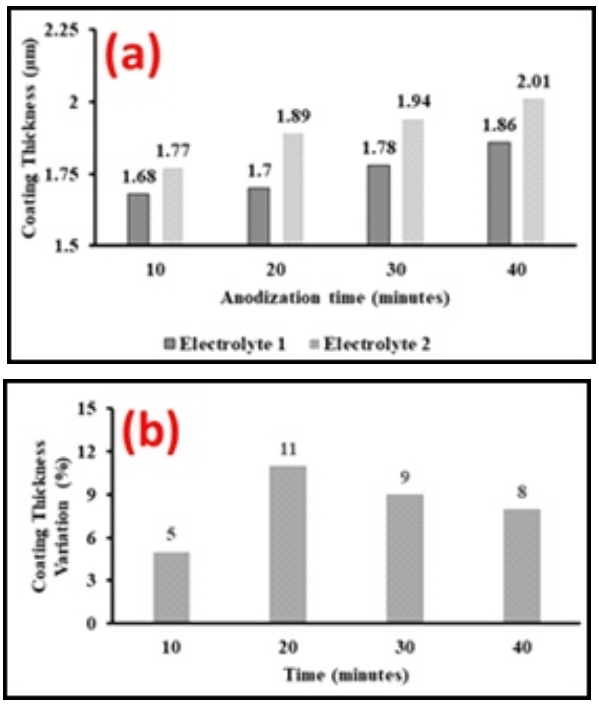

Figure 5: Anodized coating thickness (a) comparison in two different electrolytes and (b) percentage thickness variation

It can clearly be seen from the figure 5a that the coating thickness of anodized substrate in electrolyte 2 is more than in electrolyte 1 at all the four different processing times and at constant voltage of 20V. There is a consistent increase of coating thickness with an increase of time form10 minutes to 40 minutes with an interval of 10 minutes. In electrolyte 1, at 10 minutes of processing time, the anodic film developed with a thickness of about 1.68 m. With increasing the treatment time to 20 minutes, the film thickness increases to about 1.70 m which is a slight increase of about 1.2%. The treatment time increase to 30 minutes, the thickness of anodic film also increases to about 1.78 m which is about 5%. The increasing trend of thickness continues to 1.86 m which is about 4%, a slight decrease in percentage. Similar kind of trend was observed with electrolyte 2; showing initial increase in coating thickness of 7% with 20 minutes and then 3 % and 4% with 30 and 40 minutes of time respectively. Figure 5(b) showed a comparison of percentage coating thickness

variation with electrolyte 1 and 2. There is a sudden increase in coating variation from 10 to 20 minutes but the trend was then almost consistent from 20 to 40 minutes. This shows that as the time increases, thickness of coating also increases which can be seen in Figure 2a and Figure 2b [33, 35].

Comparing both electrolytes, the anodic film formed in electrolyte 2 with the processing time of 30 minutes and 40 minutes comprised of higher thickness of anodic layer as compared to electrolyte 1 with processing time 30 minutes and 40 minutes. It means that the thickness of anodic film formed in electrolyte 2 is more compact as compared to that of formed in electrolyte 1. It can also be seen in figure 5 (b) that initially the coating thickness difference is less for 10 minutes and is because of the surface buildup on the magnesium alloy and with 40 minutes the variation is high because of the formation of MgO and $Mg(OH)_2$ as the anodized layer. And further variation is the formation of cracks and oxide layers.

3.4 Corrosion Behavior of Anodized Layer:

The Nyquist impedance plots of the anodized samples in the simulated body fluids for anodized sample in electrolyte 1 at two different processing times are shown in Figure. 6.

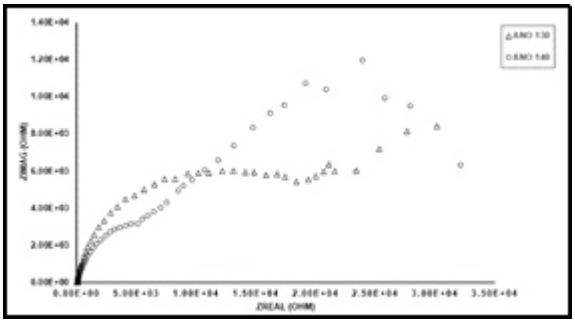

Figure 6: Nyquist Plots of anodized coating at 20V in electrolyte 1 at treatment time of 30 minutes (Ano130) and 40 minutes (Ano140)

The impedance plot of the anodic film formed by electrolyte 1 at different times displayed the capacitive arc followed by a possible second arc. The first arc may arise from the anodic film formed. Whereas, the second arc formed is might be influenced by a diffusion process [36]. The diameter of the capacitive arc of a measured Nyquist plot is closely associated with the corrosion rate [37], the larger the arc is, the better the corrosion resistance is. It can be seen in Figure 6; the corrosion resistance, of the anodized films, is improved with the increase in processing time. When the treatment time is 40 minutes, the diameter of the capacitive arc is higher as compared to that of having the processing time of 30 minutes, thus showing a higher corrosion resistance. This higher corrosion resistance is due to more thick anodic film comprising of small number of pores formed with processing time of 40 minutes in electrolyte 1.

The Nyquist impedance plots of the anodized samples in the simulated body fluids in electrolyte 2 at two different times are shown in Figure 7.

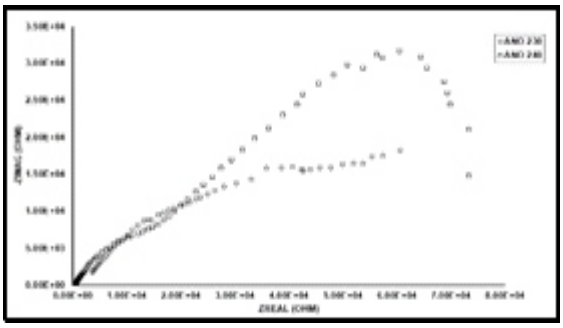

Figure 7: Nyquist Plots of anodized coating at 20V in electrolyte 2 at different treatment time (30 min and 40 min)

It can also be shown in Figure7; the corrosion resistance of the anodized layers becomes enhanced with the increase in processing time. When the treatment time is 40 minutes, the diameter of the capacitive arc is higher as compared to that of having the processing time of 30 minutes, thus displaying a higher corrosion resistance. This higher corrosion resistance is due to denser anodic film comprising of micro-cracks formed with processing time of 40 minutes in electrolyte 2. Comparing both impedance plots of anodic films formed by two electrolytes are shown in Figure 8.

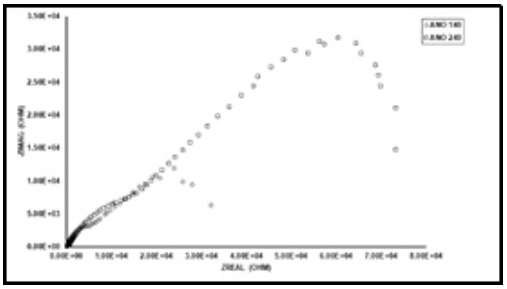

Figure 8: Nyquist Plots of anodized coating at 20V

in both electrolytes at treatment time of 40 minutes

It can be seen that the corrosion resistance of the anodized film formed in electrolyte 2 is higher as compared to that of formed in electrolyte 1. The diameter of the capacitive arc formed in electrolyte 2 is higher as compared to that of capacitive arc formed in electrolyte 1 showing higher corrosion resistance. This higher corrosion resistance is due to denser and uniform anodic film formed in electrolyte 2.

4. Conclusion:

Anodic films were produced on AZ31B magnesium alloy by anodization in electrolyte 1 and electrolyte 2 by varying the treatment time. The treatment time primarily affected surface morphology. Scanning electron microscopy revealed that electrolyte 1 resulted in less dense and non-uniform anodized film having pores (both small and larger sized) as compared to that of electrolyte 1. Whereas, electrolyte 2 resulted in compact and denser film as compared to that of formed in electrolyte 1 showing micro-cracks on the surface but decreased pore size. The biodegradation of the anodic layers was due to these pores and micro-cracks. EDS analysis of anodized film formed by electrolyte 2 revealed higher percentages of magnesium and oxygen indicating the bulk presence of MgO and $Mg(OH)_2$ as compared to film formed by electrolyte 1. The electrolyte 2 formed denser and thicker layer as compared to film formed by electrolyte 1. The results obtained by the impedance plots are in a good agreement with the analyses of surface morphology. The anodic film formed by electrolyte 2 provided the best corrosion resistance with the processing time of 40 minutes.

References:

1. B. Basu, D. S. Katti, and A. Kumar, *Advanced Biomaterials: Fundamentals, Processing, and Applications*: Wiley, 2010.
2. G. O. Hofmann, "Biodegradable implants in traumatology: a review on the state-of-the-art," *Archives of Orthopaedic and Trauma Surgery,* vol. 114, pp. 123-132, 1995/04/01 1995.
3. L. Claes and A. Ignatius, "Entwicklung neuer biodegradabler Implantate," *Der Chirurg,* vol. 73, pp. 990-996, 2002/10/01 2002.
4. F. Witte, V. Kaese, H. Haferkamp, E. Switzer, A. Meyer-Lindenberg, C. J. Wirth*, et al.*, "In vivo corrosion of four magnesium alloys and the associated bone response," *Biomaterials,* vol. 26, pp. 3557-3563, 2005/06/01/ 2005.
5. N. von der Höh, A. Krause, C. Hackenbroich, D. Bormann, A. Lucas, and A. Meyer-Lindenberg, "[Influence of different surface machining treatments of resorbable implants made from different magnesium-calcium alloys on their degradation--a pilot study in rabbit models]," *Dtsch Tierarztl Wochenschr,* vol. 113, pp. 439-46, Dec 2006.
6. L. A. de Oliveira, R. M. P. da Silva, A. C. D. Rodas, R. M. Souto, and R. A. Antunes, "Surface chemistry, film morphology, local electrochemical behavior and cytotoxic response of anodized AZ31B magnesium alloy," *Journal of Materials Research and Technology,* vol. 9, pp. 14754-14770, 2020/11/01/ 2020.
7. R. Zeng, W. Dietzel, F. Witte, N. Hort, and C. Blawert, "Progress and challenge for magnesium alloys as biomaterials," *Advanced Engineering Materials,* vol. 10, pp. B3-B14, 2008.
8. G. Song, "Control of biodegradation of biocompatable magnesium alloys," *Corrosion science,* vol. 49, pp. 1696-1701, 2007.
9. D. Zhao, F. Witte, F. Lu, J. Wang, J. Li, and L. Qin, "Current status on clinical applications of magnesium-based orthopaedic implants: A review from clinical translational perspective," *Biomaterials,* vol. 112, pp. 287-302, 2017.
10. X. Li, X. Liu, S. Wu, K. Yeung, Y. Zheng, and P. K. Chu, "Design of magnesium alloys with controllable degradation for biomedical implants: From bulk to surface," *Acta biomaterialia,* vol. 45, pp. 2-30, 2016.
11. S. Agarwal, J. Curtin, B. Duffy, and S.

Jaiswal, "Biodegradable magnesium alloys for orthopaedic applications: A review on corrosion, biocompatibility and surface modifications," *Materials Science and Engineering: C,* vol. 68, pp. 948-963, 2016.

12. L. A. d. Oliveira, R. M. P. d. Silva, and R. A. Antunes, "Scanning Electrochemical Microscopy (SECM) Study of the Electrochemical Behavior of Anodized AZ31B Magnesium Alloy in Simulated Body Fluid," *Materials Research,* vol. 22, 2019.
13. R. Erbel, C. Di Mario, J. Bartunek, J. Bonnier, B. de Bruyne, F. R. Eberli*, et al.*, "Temporary scaffolding of coronary arteries with bioabsorbable magnesium stents: a prospective, non-randomised multicentre trial," *The Lancet,* vol. 369, pp. 1869-1875, 2007/06/02/ 2007.
14. M. Esmaily, J. E. Svensson, S. Fajardo, N. Birbilis, G. S. Frankel, S. Virtanen*, et al.*, "Fundamentals and advances in magnesium alloy corrosion," *Progress in Materials Science,* vol. 89, pp. 92-193, 2017/08/01/ 2017.
15. W. D. Mueller, M. Lucia Nascimento, and M. F. Lorenzo de Mele, "Critical discussion of the results from different corrosion studies of Mg and Mg alloys for biomaterial applications," *Acta Biomater,* vol. 6, pp. 1749-55, May 2010.
16. Y. Xin, T. Hu, and P. K. Chu, "In vitro studies of biomedical magnesium alloys in a simulated physiological environment: a review," *Acta Biomater,* vol. 7, pp. 1452-9, Apr 2011.
17. F. Witte, J. Fischer, J. Nellesen, C. Vogt, J. Vogt, T. Donath*, et al.*, "In vivo corrosion and corrosion protection of magnesium alloy LAE442," *Acta Biomaterialia,* vol. 6, pp. 1792-1799, 2010/05/01/ 2010.
18. J. Kuhlmann, I. Bartsch, E. Willbold, S. Schuchardt, O. Holz, N. Hort*, et al.*, "Fast escape of hydrogen from gas cavities around corroding magnesium implants," *Acta Biomaterialia,* vol. 9, pp. 8714-8721, 2013/11/01/ 2013.
19. U. M. Tefashe, M. E. Snowden, P. D. Ducharme, M. Danaie, G. A. Botton, and J. Mauzeroll, "Local flux of hydrogen from magnesium alloy corrosion investigated by scanning electrochemical microscopy," *Journal of Electroanalytical Chemistry,* vol. 720-721, pp. 121-127, 2014/04/15/ 2014.
20. M. Pogorielov, E. Husak, A. Solodivnik, and S. Zhdanov, "Magnesium-based biodegradable alloys: Degradation, application, and alloying elements," *Interv Med Appl Sci,* vol. 9, pp. 27-38, Mar 2017.
21. H. Hornberger, S. Virtanen, and A. R. Boccaccini, "Biomedical coatings on magnesium alloys A review," *Acta Biomaterialia,* vol. 8, pp. 2442-2455, 2012/07/01/ 2012.
22. A. F. Cipriano, J. Lin, C. Miller, A. Lin, M. C. Cortez Alcaraz, P. Soria*, et al.*, "Anodization of magnesium for biomedical applications Processing, characterization, degradation and cytocompatibility," *Acta Biomaterialia,* vol. 62, pp. 397-417, 2017/10/15/ 2017.
23. H. Fukuda and Y. Matsumoto, "Effects of Na2SiO3 on anodization of MgAlZn alloy in 3 M KOH solution," *Corrosion Science,* vol. 46, pp. 2135-2142, 2004/09/01/ 2004.
24. R. F. Zhang, D. Y. Shan, R. S. Chen, and E. H. Han, "Effects of electric parameters on properties of anodic coatings formed on magnesium alloys," *Materials Chemistry and Physics,* vol. 107, pp. 356-363, 2008/02/15/ 2008.
25. W. Ximei, Z. Liqun, L. Huicong, and L. Weiping, "Influence of surface pretreatment on the anodizing film of Mg alloy and the mechanism of the ultrasound during the pretreatment," *Surface and Coatings Technology,* vol. 202, pp. 4210-4217, 2008/05/25/ 2008.
26. V. Ezhilselvi, J. Nithin, J. N. Balaraju, and S. Subramanian, "The influence of current density on the morphology and corrosion properties of MAO coatings on AZ31B

magnesium alloy," *Surface and Coatings Technology,* vol. 288, pp. 221-229, 2016/02/25/ 2016.

27. S.-N. Pak, Z. Jiang, Z. Yao, J.-M. Ju, K.-S. Ju, and U.-J. Pak, "Fabrication of environmentally friendly anti-corrosive composite coatings on AZ31B Mg alloy by plasma electrolytic oxidation and phytic acid/3-aminopropyltrimethoxysilane post treatment," *Surface and Coatings Technology,* vol. 325, pp. 579-587, 2017/09/25/ 2017.
28. T. Lei, C. Ouyang, W. Tang, L.-F. Li, and L.-S. Zhou, "Enhanced corrosion protection of MgO coatings on magnesium alloy deposited by an anodic electrodeposition process," *Corrosion science,* vol. 52, pp. 3504-3508, 2010.
29. T. Lei, C. Ouyang, W. Tang, L.-F. Li, and L.-S. Zhou, "Preparation of MgO coatings on magnesium alloys for corrosion protection," *Surface and Coatings Technology,* vol. 204, pp. 3798-3803, 2010.
30. D. Xue, Y. Yun, M. J. Schulz, and V. Shanov, "Corrosion protection of biodegradable magnesium implants using anodization," *Materials Science and Engineering: C,* vol. 31, pp. 215-223, 2011.
31. L. Chai, X. Yu, Z. Yang, Y. Wang, and M. Okido, "Anodizing of magnesium alloy AZ31 in alkaline solutions with silicate under continuous sparking," *Corrosion Science,* vol. 50, pp. 3274-3279, 2008.
32. F. H. Muhammad Umar Manzoor, Hafsa Zafar, Hamna Sajjad, Asma Salman, Fahad Riaz, Ameeq Farooq, Tahir Ahmad, Muhammad Kamran, "Electrochemical Characterization of AlTiN Coating on Stainless Steel Substrate for Biomedical Implant," *Journal of the Pakistan Institute of Chemical Engineers,* vol. 48, p. 8, 2021 2020.
33. L.-L. Li, Y.-L. Cheng, H.-M. Wang, and Z. Zhang, "Anodization of AZ91 magnesium alloy in alkaline solution containing silicate and corrosion properties of anodized films," *Transactions of Nonferrous Metals Society of China,* vol. 18, pp. 722-727, 2008.
34. G. Zhang, L. Wu, A. Tang, B. Weng, A. Atrens, S. Ma*, et al.*, "Sealing of anodized magnesium alloy AZ31 with MgAl layered double hydroxides layers," *RSC advances,* vol. 8, pp. 2248-2259, 2018.
35. J. S. Li and J. Q. Liu, "Structure and Properties of Anodized Films Formed on AZ91D Magnesium Alloy," in *Applied Mechanics and Materials*, 2011, pp. 1586-1591.
36. M. Alvarez-Lopez, M. D. Pereda, J. Del Valle, M. Fernandez-Lorenzo, M. Garcia-Alonso, O. A. Ruano*, et al.*, "Corrosion behaviour of AZ31 magnesium alloy with different grain sizes in simulated biological fluids," *Acta biomaterialia,* vol. 6, pp. 1763-1771, 2010.
37. G. Song, A. L. Bowles, and D. H. StJohn, "Corrosion resistance of aged die cast magnesium alloy AZ91D," *Materials Science and Engineering: A,* vol. 366, pp. 74-86, 2004.